PAPER • **OPEN ACCESS**

Atomistic simulations of hydrogen and carbon segregation in α-iron grain boundaries

To cite this article: Mohamed H Hamza *et al* 2019 *IOP Conf. Ser.: Mater. Sci. Eng.* **610** 012009

IOP Conf. Series: Materials Science and Engineering **610** (2019) 012009 doi:10.1088/1757-899X/610/1/012009

Atomistic simulations of hydrogen and carbon segregation in α-iron grain boundaries

Mohamed H Hamza[1,2], Mohamed A Hendy[1] and Tarek M. Hatem[1,3,4]

[1] Centre for Simulation Innovation and Advanced Manufacturing, the British University in Egypt, El-Sherouk City, Cairo 11837, Egypt
[2] Department of Mechanical Engineering, Johns Hopkins University, Baltimore, Maryland 21218, USA
[3] Faculty of Energy and Environmental Engineering, the British University in Egypt, El-Sherouk City, Cairo 11837, Egypt

[4] Email: tarek.hatem@bue.edu.eg

Abstract. During material deformation, the coincidence site lattice (CSL) grain boundaries (GBs) are exhibiting deviations from their ideal lattice structure. Hence, this will change the atomic structural integrity by generating full and partial dislocation joints on the ideal CSL boundaries. In this analysis, the ideal ∑5 (310) GB structures and its angular deviations in α-iron within the limit of Brandon criterion, in order to conserve the dislocation core structure, will be studied in depth using molecular statics simulations. Firstly, the hydrogen and carbon atoms energetics within the GBs core structure and their free surfaces are calculated. Then Rice-Wang cohesive structure model is applied to compute the embrittlement/strengthening effect of the solute atoms on the ideal and deviated GB structures. Hydrogen showed significant embrittlement and degradation in the mechanical properties of α-iron, while carbon showed a desirable atomic strengthening effect.

1. Introduction

Failure modes of polycrystalline materials depend on many factors that include diffusion and segregation of solutes as well as the structure of the coincidence site lattice (CSL) grain boundaries (GBs) [1-6]. Diffused solute atoms to GBs can change the properties of the steel. Segregation of certain impurities to GBs is the main cause for intergranular fracture of steel among various other mechanisms [7-10]. The existence of these solutes impacts the tensile and ultimate strength of steel alloys. Diffused solutes to sink defects lead to improving the strength of steel, on the other hand others can affect the plasticity behaviour of steel significantly [11-13]. Many studies indicated that carbon increases the cohesion strength at GB. While the presence of hydrogen in steel have undesirable material properties effects such as; high localized plasticity and decohesion of GBs of steel [4-6].

In engineering materials, GB shows some deviation from ideal CSL configuration, either a deviation from the ideal symmetry plane or the misorientation angle exists. The deviations induce network of full and partial dislocations at the GB [14,15]. Different deviation angle changes the optimum diffusion sites of solute atoms at the grain boundary, this was also proved experimentally using atom probe tomography for measuring carbon diffusion and segregation at deviated CSL-GBs [16,17].

2. Methodology

In order to mimic the experimental observation of the GB misorientation, the angular deviations which will be applied to ∑5 (310) GB must be defined. Brandon criterion is used to measure the maximum deviation angle where the CSL-GB structure and energy can be maintained [18]. This maximum deviation angle is calculated as follows:

$$\boldsymbol{\theta_{max}} = \boldsymbol{\theta_{\circ}}\boldsymbol{\sum^{-0.5}} \tag{1}$$

where $\boldsymbol{\theta_{max}}$ is Brandon limit for conserving the GB characteristic structure, $\boldsymbol{\theta_{\circ}}$ is an imperial constant which is ~15° and ∑ is the CSL density. The illustration of the deviation from the ideal CSL-GB is shown in figure 1. $\boldsymbol{\theta}$ indicates the misorientation symmetry angle between the two grains and $\boldsymbol{\phi}$ is the deviation angle.

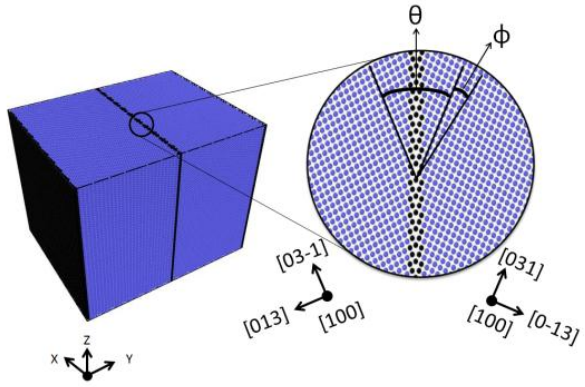

Figure 1. ∑5 (310) GB structure (left)
deviating angle convept (right)

Rice-Wang model [19-21] is used to estimate the embrittlement/strengthening effect of hydrogen and carbon segregation to ∑5 (310) GB and its deviant configurations. According to the aforementioned model, the ability of either interstitial or substitutional atom to reduce the Griffith work of a GB is a proportional to the cohesive energies at the GB and free surface of this solute atom. The strengthening impact or embrittlement tendency can be then computed as follows:

$$\boldsymbol{E^{\alpha}_{SE}} = \boldsymbol{E^{\alpha}_{seg\ FS}} - \boldsymbol{E^{\alpha}_{seg\ GB}} \tag{2}$$

where $\boldsymbol{E^{\alpha}_{SE}}$ is the strengthening energy due to impurity atom segregating to GB, $\boldsymbol{E^{\alpha}_{seg\ FS}}$ is the surface segregation and $\boldsymbol{E^{\alpha}_{seg\ GB}}$ is GB segregation. For the case where the value of $\boldsymbol{E^{\alpha}_{SE}}$ is positive, the solute atom enhances the cohesive strength of the grain boundary and vice versa. Hence positive values of $\boldsymbol{E^{\alpha}_{SE}}$ indicates a solute strengthening effect for the iron atoms at the GB, while negative values indicate embrittlement effect.

Atomistic statics simulations are used to quantify the segregation energy of a single interstitial/substitutional atom (hydrogen/carbon) at the trapping sites along the GB ideal plane and the corresponding free surface. For each GB structure, the interstitial/substitutional atom segregation energy to GB within -15 to 15 Angstroms from the ideal symmetry plane and the surface segregation energy corresponding to each GB are computed. The following equations are used to calculate GB and surface segregation.

$$\boldsymbol{E^{\alpha}_{seg\ GB}} = (\boldsymbol{E^{\alpha}_{GB}} - \boldsymbol{E_{GB}}) - (\boldsymbol{E^{\alpha}_{bulk}} - \boldsymbol{E_{bulk}}) \tag{3}$$

$$\boldsymbol{E^{\alpha}_{seg\ FS}} = (\boldsymbol{E^{\alpha}_{FS}} - \boldsymbol{E_{FS}}) - (\boldsymbol{E^{\alpha}_{bulk}} - \boldsymbol{E_{bulk}}) \tag{4}$$

3. Results

The H/C-segregation energy effect as a function of position from ∑5 (310) GB as calculated from equation (3) is shown in figures. 2&3. For this studied GB, it is clear that the ideal GB and the deviated cases are preferable sites for hydrogen/Carbon diffusion and act as solute sink compared to the bulk structure. Moreover, as the angular deviations **ϕ** increases, the GB absorption length for H increases, while no significant changes noticed for carbon atoms due to larger distortion elastic filed of carbon, compared to hydrogen atoms. The aforementioned length measures the GB effective distance at which the H/C-atoms located at the tetrahedral/octahedral sites respectively can change the GB atomic bonding.

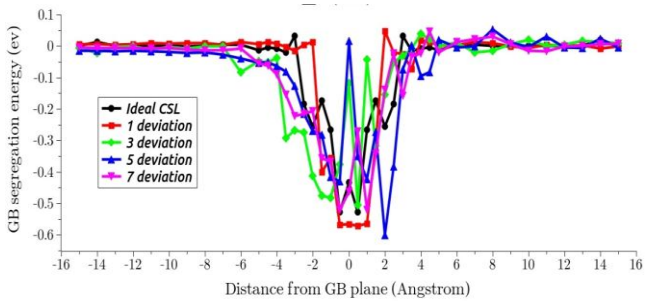

Figure 2: Hydrogen GB segregation energy of the ideal and deviant ∑5 (310) configurations

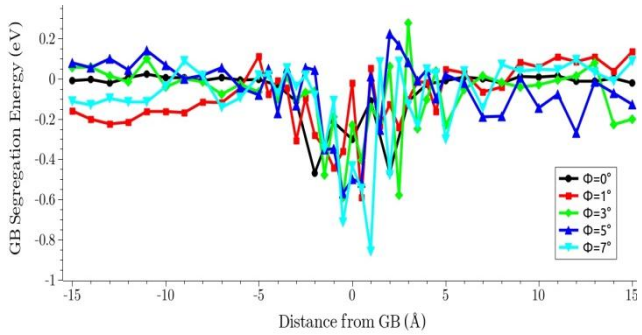

Figure 3: Carbon GB segregation energy of the ideal and deviant ∑5 (310) configurations

The effect of ϕ on the H/C-segregation energy within a layer of 2 Angstroms from the GB plane can be deduced from figures. 2&3 for the ideal and deviated CSL-GBs structures. The segregation energies summarized in the paper are average values based on 95% confidence interval. ∑5 (310) GB shows a low sensitivity for varying ϕ on H-GB segregation; where it is approximately constant in the studied range $0° \leq (\phi) \leq 7°$ with average value of ~ -0.34 eV. For carbon segregation energy, the values of segregation at the deviation angles are higher, in absolute terms, which indicates lower impact on the atomic bonding in the GB structure compared to H. Additionally, low C-segregation sensitivity is observed as well with average value of ~ -0.26 eV. However, a difference between the ideal and deviated structure can be observed for both carbon and hydrogen segregation.

By calculating the GB and free surface segregation energies as shown in above, the effect of hydrogen and carbon atoms on the GB cohesion strength can be evaluated. Generally, interstitial or

substitutional atoms segregate at a GB can deteriorate or enhance the GB-cohesive energy depending on the resulting stress filed interactions. In order to compute the impact of the deviation from the ideal GB configuration on the tendency to H-embrittlement or GB strengthening, GB-cohesive energy is predicted using Rice-Wang model [21] as follows:

$$2\boldsymbol{\gamma_{int}} = (\boldsymbol{2\gamma_{int}})_{\mathbf{0}} - (\boldsymbol{E^{\alpha}_{seg\ GB}} - \boldsymbol{E^{\alpha}_{seg\ FS}})\,\tau \quad (5)$$

where $2\boldsymbol{\gamma_{int}}$ is the GB-cohesion energy due to solute atoms segregation, $(\boldsymbol{2\gamma_{int}})_{\mathbf{0}}$ is the cohesion energy of the pure GB, and τ is a fitting constant. The change of the GB cohesive energy along with the deviation angle ϕ for the studied configurations is shown in figure (4).

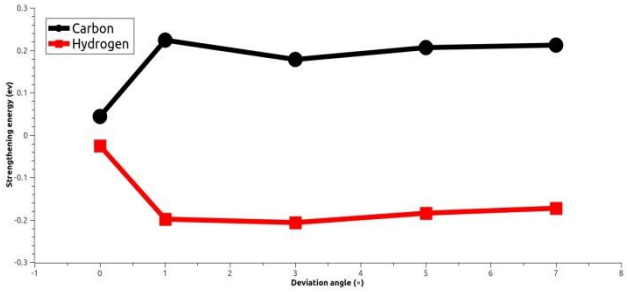

Figure 4: Change in cohesive energy vs. deviation angle of GB

As shown in figure (4) H reduces the cohesive energy and subsequently initiates intergranular fracture within these studied interfaces. This is due to the fact that hydrogen is more energy favourable in free surfaces sites than of the GB core sites, therefore, the Griffith work for brittle deformation behaviour is reduced and intergranular failure mode is experienced in a more frequent manner [22-24]. For carbon segregation within the investigated GBs; it can be shown that increasing the deviation angle up to 3° is sufficient to increase the cohesive strength considerably with regards to the ideal structure. However, the difference between the deviant structures is minor. Hence it can be concluded that for ∑5 (310) GB, all deviation angles have beneficial strengthening effect on the cohesive energy due to carbon existence, while H showed an embrittlement effect compared to the ideal GB interface.

4. Conclusion

H/C segregation within the ∑5 (310) GB in $\boldsymbol{\alpha}$-iron structures is investigated through using molecular statics simulations. The results showed that the angular deviations from the ideal CSL-GBs are affecting significantly the H/C atomic bonding behaviour within the boundaries. H is showing significant embrittlement effect due to decreasing the atomic bonding between iron atoms at the GB and with more deviation upon 3° from the ideal GB configuration, slightly more cohesion degradation is observed. On the other hand, C is showing beneficial atomic bonding strengthening at the iron atoms located at the GB interface. This is due to the increase in the iron cohesive strength, however there is no significant effect with increasing the deviation angle upon 3° from the ideal GB structure. This can be used to infer that with slight atomic deviations, C atoms can have significant increase on the iron toughness and improve its overall deformability properties. While H atoms will show decrease in iron toughness, also more brittle iron behaviour will be observed with increasing the deviation angle. Hence, careful consideration is needed during recrystallization processing to produce iron resistant to hydrogen embrittlement and iron strengthened by carbon segregation.

Acknowledgments

This project is funded by the Academy of Scientific Research and Technology (ASRT) under Joint Collaborative Efforts of Egyptians Expatriates & Scientific Organizations towards Tackling R&D Challenges (JESOR), Contract No. 17.

References

[1] Hatem, T. M., & Zikry, M. A. (2010). Deformation and failure of single-packets in martensitic steels. Computers, Materials and Continua, 17(2), 127–147.
[2] Shanthraj, P., Hatem, T. M., & Zikry, M. A. (2011). Microstructural modeling of failure modes in martensitic steel alloys. In Materials Research Society Symposium Proceedings (Vol. 1296, pp. 56–61). http://doi.org/10.1557/opl.2011.1446
[3] Hatem, T. M., & Zikry, M. A. (2010). Dynamic shear-strain localization and inclusion effects in lath martensitic steels subjected to high pressure loads. Journal of the Mechanics and Physics of Solids, 58(8), 1057–1072. http://doi.org/10.1016/j.jmps.2010.04.009
[4] Wagih, M., Tang, Y., Hatem, T., & El-Awady, J. A. (2015). Discerning enhanced dislocation plasticity in hydrogen-charged α-iron nano-crystals. Materials Research Letters, 3(4), 184–189. http://doi.org/10.1080/21663831.2015.1052889
[5] Hamza, M., Hatem, T. M., Raabe, D., & El-Awady, J. A. (2015). Hydrogen diffusion and segregation in alpha iron ∑ 3 (111) grain boundaries. In ASME International Mechanical Engineering Congress and Exposition, Proceedings (IMECE) (Vol. 9–2015). http://doi.org/10.1115/IMECE2015-53118
[6] Shi, J., Zikry, M., & Hatem, T. M. (2006). Inelastic behavior and grain-boundary effects in polycrystalline materials. In Materials Research Society Symposium Proceedings (Vol. 978, pp. 333–338).
[7] Hatem, T. M., & Zikry, M. A. (2009). Shear pipe effects and dynamic shear-strain localization in martensitic steels. Acta Materialia, 57(15), 4558–4567. http://doi.org/10.1016/j.actamat.2009.06.028
[8] Shi, J., Zikry, M. A., & Hatem, T. M. (2008). Microstructural modeling of failure in polycrystalline materials. In Advances in Heterogeneous Material Mechanics 2008 - Proceedings of the 2nd International Conference on Heterogeneous Material Mechanics, ICHMM 2008 (pp. 3–8).
[9] Hatem, T. M., & Zikry, M. A. (2009). Dislocation density crystalline plasticity modeling of lath martensitic microstructures in steel alloys. Philosophical Magazine, 89(33), 3087–3109. http://doi.org/10.1080/14786430903185999
[10] Hatem, T. M., & Zikry, M. A. (2009). Microstructural modelling of failure modes in crystalline materials. In Computational Plasticity X - Fundamentals and Applications.
[11] Herbig M, Raabe D, Li YJ, Choi P, Zaefferer S, Goto S. Atomic-Scale Quantification of Grain Boundary Segregation in Nanocrystalline Material. Phys Rev Lett 2014;126103:1–5. doi:10.1103/PhysRevLett.112.126103.
[12] Hatem, T. M., & Zikry, M. A. (2010). Deformation and failure of single-packets in martensitic steels. Computers, Materials and Continua, 17(2), 127–147.
[13] Khafagy, K. H., Hatem, T. M., & Bedair, S. M. (2018). Three-dimensional crystal-plasticity based model for intrinsic stresses in multi-junction photovoltaic. Minerals, Metals and Materials Series (Vol. Part F6). http://doi.org/10.1007/978-3-319-72362-4_41
[14] Solanki KN, Tschopp MA, Bhatia MA, Rhodes NR. Atomistic investigation of the role of grain boundary structure on hydrogen segregation and embrittlement in α-Fe. Metall Mater Trans A Phys Metall Mater Sci 2013;44:1365–75. doi:10.1007/s11661-012-1430-z.
[15] Hatem, T. M., & Zikry, M. A. (2009). Microstructural modelling of failure modes in crystalline materials. In 12th International Conference on Fracture 2009, ICF-12 (Vol. 8, pp. 5923–5932).
[16] Shanthraj, P., Hatem, T. M., & Zikry, M. A. (2011). Microstructural modeling of failure modes in martensitic steel alloys. In Materials Research Society Symposium Proceedings (Vol. 1296, pp. 56–61). http://doi.org/10.1557/opl.2011.1446
[17] Hatem, T. M., & Zikry, M. A. (2011). A model for determining initial dislocation densities associated with martensitic transformations. Materials Science and Technology, 27(10), 1570–1573. http://doi.org/10.1179/1743284711Y.0000000079

[18] Khafagy, K. H., Hatem, T. M., & Bedair, S. M. (2018). Impact of embedded voids on thin-films with high thermal expansion coefficients mismatch. Applied Physics Letters, 112(4). http://doi.org/10.1063/1.5011394
[19] Palumbo G, Aust KT, Lehockey EM, Erb U, Lin P. On a More Restrictive Geometric Criterion for "Special" CSL Grain Boundaries. Scr Mater 1998;38:1685–90. doi:https://doi.org/10.1016/S1359-6462(98)00077-3.
[20] Read WT, Shockley W. Dislocation Models of Crystal Grain Boundaries. Phys Rev 1950;78:275–89. doi:10.1103/PhysRev.78.275.
[21] Rice JR, Wang JS. Embrittlement of interfaces by solute segregation. Mater Sci Eng A 1989;107:23–40. doi:10.1016/0921-5093(89)90372-9.
[22] Khafagy, K.H., Hatem, T.M. and Bedair, S.M., Modelling of III-Nitride Epitaxial Layers Grown on Silicon Substrates with Low Dislocation-Densities. MRS Advances, pp.1-6.
[23] Hendy, M.A., Hatem, T.M. and El-Awady, J.A., 2018. Atomistic Simulations of Carbon and Hydrogen Diffusion and Segregation in Alfa-Iron Deviant CSL Grain Boundaries. MRS Advances, 3(45-46), pp.2795-2800.
[24] Hamza, M.H., Hendy, M.A., Hatem, T.M. and El-Awady, J.A., 2018. Impact of angular deviation from coincidence site lattice grain boundaries on hydrogen segregation and diffusion in α-iron. MRS Communications, 8(3), pp.1197-1203.